

The Physics of Lightning

V. A. Rakov

Received: 19 October 2012 / Accepted: 26 March 2013 / Published online: 16 April 2013
© Springer Science+Business Media Dordrecht 2013

Abstract An overview of the physics of cloud-to-ground lightning is given, including its initiation, propagation, and attachment to ground. Discharges artificially initiated (triggered) from natural thunderclouds using the rocket-and-wire technique are discussed with a view toward studying properties of natural lightning. Both conventional and runaway breakdown mechanisms of lightning initiation in thunderclouds are reviewed, as is the role of the lower positive charge region in facilitating different types of lightning. New observations of negative-leader stepping and its attachment to ground are compared to similar processes in long laboratory sparks. The mechanism and parameters of compact intracloud lightning discharges that are thought to be the most intense natural producers of HF-VHF (3–300 MHz) radiation on Earth are reviewed. The M-component mode of charge transfer to ground and its difference from the leader/return-stroke mode are discussed. Lightning interaction with the ionosphere and the production of energetic radiation (X-rays and gamma radiation) by cloud-to-ground leaders are considered.

Keywords Lightning · Initiation mechanism · Conventional breakdown · Relativistic runaway breakdown · Cold runaway breakdown · Lower positive charge region · Compact intracloud discharges · Leader stepping · Attachment process · M-components · Ionosphere · X-rays · Gamma radiation

1 An Overview

About 90 % or more of global cloud-to-ground lightning is accounted for by negative (negative charge is effectively transported to the ground) downward (the initial process begins in the cloud and develops in the downward direction) lightning. Other types of cloud-to-ground lightning include positive downward, negative upward, and positive upward discharges. There are also bipolar lightning discharges sequentially transferring to ground both positive and negative charges during the same flash. It is worth noting that

V. A. Rakov (✉)
University of Florida, 553 Engineering Bldg. #33, P.O. Box 116130, Gainesville, FL 32611-6130, USA
e-mail: rakov@ece.ufl.edu

cloud-to-ground discharges constitute only about 25 % of global lightning activity and the remaining 75 % do not involve ground. The latter are referred to as cloud discharges. The focus of this review is on negative cloud-to-ground discharges.

The source of lightning is usually a cumulonimbus (thundercloud), whose idealized charge structure is shown in Fig. 1 as three vertically stacked regions labeled “P” and “LP” for main positive and lower positive charge regions, respectively, and “N” for main negative charge region. Various processes comprising a negative cloud-to-ground lightning flash are also illustrated in Fig. 1. The basic elements of the negative downward lightning discharge are termed component strokes or just strokes. Each flash typically contains 3–5 strokes, the observed range being 1–26. Roughly half of all lightning discharges to earth strike ground at more than one point with the spatial separation between the channel terminations being up to many kilometers. A flash composed of two strokes following the same channel to ground is shown in Fig. 1. There are two major processes comprising a lightning stroke, the leader and the return stroke, which occur as a sequence with the leader preceding the return stroke. The initial (first-stroke) leader is preceded by an in-cloud process called the preliminary breakdown. There is no consensus on the mechanism of this process. It may be a discharge bridging the main negative and the lower positive charge regions, as shown in Fig. 1.

The leader creates a conducting path between the negative cloud charge source region and ground and distributes negative charge from the cloud source region along this path,

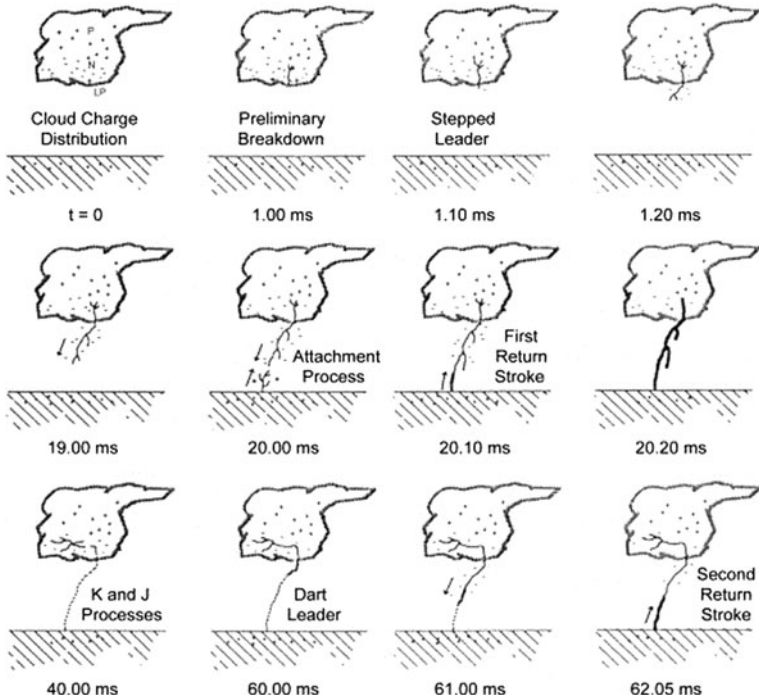


Fig. 1 Various processes comprising a negative cloud-to-ground lightning flash. Time labels below the sketches can be used to roughly estimate typical durations of the processes and time intervals between them ($t = 0$ corresponds to the beginning of preliminary breakdown process which ends at $t = 1$ ms). Continuing current and M-components are not illustrated in this Figure. Taken from Rakov and Uman (2003)

and the return stroke traverses that path moving from ground toward the cloud charge source region and neutralizes the negative-leader charge. Thus, both leader and return-stroke processes serve to effectively transport negative charge from the cloud to ground. The leader initiating the first return stroke differs from the leaders initiating subsequent strokes (all strokes other than first are termed subsequent strokes). In particular, the first-stroke leader appears optically to be an intermittent process, hence the term stepped leader, while the tip of a subsequent-stroke leader appears to move continuously. The continuously moving subsequent-stroke leader tip appears on streak photographs as a downward-moving “dart”, hence the term dart leader. The apparent difference between the two types of leaders is related to the fact that the stepped leader develops in virgin air, while the dart leader follows the “pre-conditioned” path of the preceding stroke or strokes. Sometimes a subsequent leader exhibits stepping while propagating along a previously formed channel; it is referred to as dart-stepped leader.

When the descending stepped leader attaches to the ground, the first return stroke begins. The first return-stroke current measured at ground typically rises to an initial peak of about 30 kA in some microseconds and decays to half-peak value in some tens of microseconds. The return stroke effectively lowers to ground the several coulombs of charge originally deposited on the stepped-leader channel including all the branches.

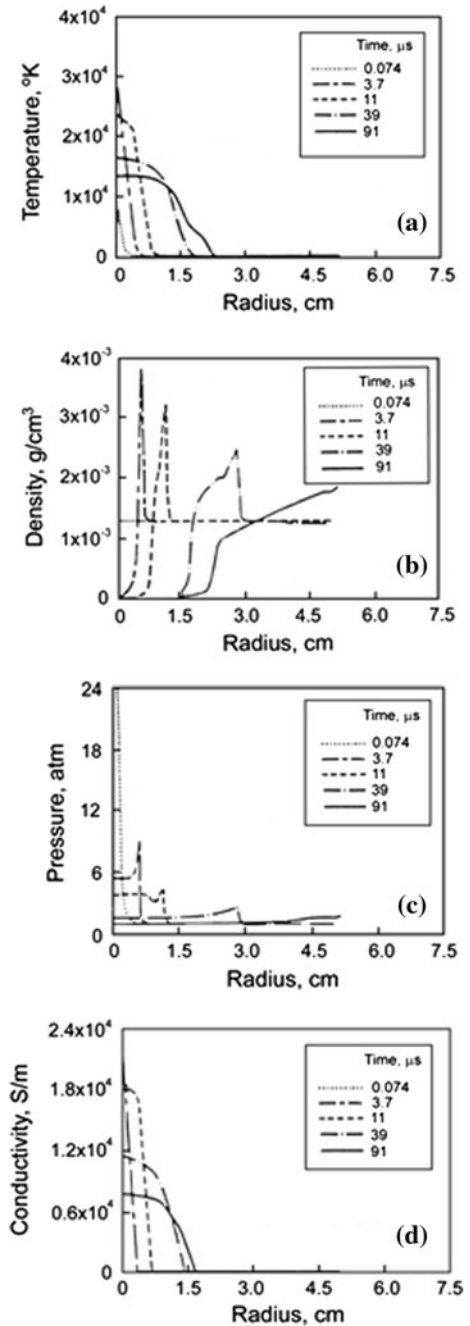
When the first return stroke, including any associated continuing current (discussed below) and in-cloud discharge activity ceases, the flash may end. In this case, the lightning is called a single-stroke flash. However, more often the residual first-stroke channel is traversed by one or more dart-leader/return-stroke sequences. During the time interval between the end of the first return stroke and the initiation of a dart leader, J (for junction) and K processes occur in the cloud. The K in the term K-change stands either for Kleine (German for small) or for N. Kitagawa and M. Kobayashi who were the first to study this lightning process in detail (Brook and Ogawa 1977). K processes can be viewed as transients occurring during the slower J process. Both the J processes and the K processes in cloud-to-ground discharges serve to transport additional negative charge into and along the existing channel (or its remnants), although not all the way to the ground.

Once the bottom of the dart-leader channel is connected to the ground, the second (or any subsequent) return-stroke wave is launched upward, which again serves to neutralize the leader charge. The subsequent return-stroke current at ground typically rises to a peak value of 10–15 kA in less than a microsecond and decays to half-peak value in a few tens of microseconds.

The high-current return-stroke wave rapidly heats the channel to a peak temperature near or above 30,000 °K and creates a channel pressure of 10 atm or more, resulting in channel expansion, intense optical radiation, and an outward propagating shock wave that eventually becomes the thunder (sound wave) we hear at a distance. Figure 2 shows the temperature, mass density, pressure, and electrical conductivity versus radial distance from the channel axis at five instants of time ranging from 0.074 to 91 μ s, all predicted by the gas-dynamic model of Paxton et al. (1986). The input current for the model linearly increased to 20 kA in 5 μ s and thereafter exponentially decayed with a time constant of 50 μ s. Return-stroke input energy estimates predicted by various gas-dynamic models are of the order of 10^3 J/m, consistent with experimental estimates for rocket-triggered lightning (Jayakumar et al. 2006), but about two orders of magnitude lower than an estimate of Krider et al. (1968), obtained from comparison of the optical radiation produced by lightning with that of a laboratory spark of known input energy.

The impulsive component of the current in a return stroke is often followed by a continuing current which has a magnitude of tens to hundreds of amperes and a duration up

Fig. 2 **a** Temperature, **b** mass density, **c** pressure, and **d** electrical conductivity each versus radius (radial distance from lightning channel axis) at five instants of time ranging from 0.074 to 91 μs , as predicted by the gas-dynamic model of Paxton et al. (1986) for an input current linearly rising to 20 kA in 5 μs and thereafter exponentially decaying with a time constant of 50 μs . Adapted from Paxton et al. (1986). According to Paxton et al. (1987), the profile at 3.7 μs should be interpreted as having a constant value equal to that at the channel axis out to a radius of 0.36 cm



to hundreds of milliseconds. Continuing currents with a duration in excess of 40 ms are traditionally termed long continuing currents. Between 30 and 50 % of all negative cloud-to-ground flashes contain long continuing currents (usually following subsequent return strokes). Current pulses superimposed on continuing currents, as well as the corresponding

enhancements in luminosity of the lightning channel, are referred to as M-components. The distinction between return-stroke current and continuing current is apparently related to the source of the charge that is transported to ground by these two lightning processes. The return stroke removes charge that has been deposited on the channel by a preceding leader, whereas continuing current is likely associated with the tapping of fresh charge regions in the cloud. It is generally thought that the maximum duration of the return-stroke stage is about 3 ms (Malan and Schonland 1951; Beasley et al. 1982; Rakov et al. 1990). The bulk of the leader charge is stored in the radial-corona sheath surrounding the relatively narrow channel core that carries longitudinal current. Pierce (1958) and Rao and Bhattacharya (1966) have estimated that the time of the collapse of the radial-corona charge during the return-stroke process is of the order of a millisecond, consistent with the assumed maximum return-stroke duration.

Lightning discharges cause a variety of transient relatively low-luminosity optical phenomena in the clear air between the cloud tops (at altitudes of near 20 km or less) and the lower ionosphere (near 60–90 km depending on the time of day). Six general types of such phenomena, collectively referred to as transient luminous events (TLEs), have been observed: red sprites, halos, blue starters, blue jets, gigantic jets, and elves. They represent a mechanism for energy transfer from lightning and the thundercloud to the regions of the atmosphere between the cloud tops and the lower ionosphere. Sprites have tens-of-kilometer vertical extent and complex spatial structures. From spatially and temporally averaged observations, they have peak optical intensities generally between 0.1 and 10 MR and overall durations from about a millisecond to many tens of milliseconds. Sprites are difficult to see, even with a dark-adapted eye. Halos are brief descending glows with lateral extent 40–70 km, which accompany or precede (but not always) more structured sprites. Blue starters and blue jets propagate upward from the cloud tops at speeds near 10^5 m/s. The lower, brightest part of blue starters and blue jets apparently can have optical intensities above 10 MR, while their tops are considerably less bright. Starters extend less than 10 km above cloud tops, generally only a few kilometers, while blue jets have vertical extents of 20 km or so. Blue starter and blue jet durations are up to a few hundreds of milliseconds. Occasionally, jet-like events propagate all the way to the ionosphere, in which case they are referred to as gigantic jets. Krehbiel et al. (2008) demonstrated that blue jets occur as a result of electrical breakdown between the upper positive charge and the negative screening charge near the cloud top. In contrast, they found the gigantic jets to begin as a normal intracloud discharge between dominant mid-level negative charge and an upper-level positive charge depleted by mixing with the negative screening charge, which continues to propagate out of the top of the thundercloud. Elves expand outward across the lower ionosphere in less than a millisecond to a maximum horizontal extent of 200–700 km and are reported to have optical intensities of roughly 1–10 MR.

Lightning can be artificially initiated (triggered) by launching of a small rocket trailing a thin grounded wire toward a charged cloud overhead. When the rocket, ascending at about 150–200 m/s, is about 200–300 m high, the field enhancement near the rocket tip launches a positively charged leader that propagates upward toward the cloud. This upward positive leader vaporizes the trailing wire, bridges the gap between the cloud and ground, and establishes an initial continuous current with a duration of some hundreds of milliseconds that transports negative charge from cloud charge source region to the triggering facility. After the cessation of the initial continuous current, one or more downward dart-leader/upward return-stroke sequences may traverse the same path to the triggering facility. The dart leaders and the following return strokes in triggered lightning are similar to dart-leader/return-stroke sequences in natural lightning, although the initial processes in natural

downward and triggered lightning are distinctly different. To date, well over 1,000 lightning discharges have been triggered all over the world using the rocket-and-wire technique, with over 400 of them at Camp Blanding, Florida (see, for example, Rakov and Uman 2003, Ch. 7). The results of triggered-lightning experiments have provided considerable insight into natural lightning processes that would not have been possible from studies of natural lightning due to its random occurrence in space and time.

A more detailed discussion of selected topics in lightning physics is presented in the following sections. These topics include initiation of lightning in thunderclouds, compact intracloud lightning discharges, negative-leader stepping process, lightning attachment process, lightning M-component mechanism, lightning interaction with the ionosphere, and X-ray production by cloud-to-ground leaders. Additional information can be found in the books authored or edited by Bazelyan and Raizer (2000), Cooray (2003), Rakov and Uman (2003), and Betz et al. (2009).

2 Initiation of Lightning in Thunderclouds

The primary source of lightning is the cloud type termed cumulonimbus, commonly referred to as the thundercloud. Maximum electric fields typically measured in thunderclouds (see Table 1 of Rakov (2006) and references therein) are $1\text{--}2 \times 10^5$ V/m (the highest measured value is 4×10^5 V/m), which is lower than the expected conventional breakdown field, of the order of 10^6 V/m. Two mechanisms of lightning initiation have been suggested. One relies on the emission of positive streamers from hydrometeors when the electric field exceeds $2.5\text{--}9.5 \times 10^5$ V/m, and the other involves high-energy cosmic ray particles and the runaway breakdown that occurs in a critical field, calculated to be about 10^5 V/m at an altitude of 6 km. Either of these two mechanisms permits, in principle, creation of an ionized region (“lightning seed”) in the cloud that is capable of locally enhancing the electric field at its extremities. Such field enhancement is likely to be the main process leading to the formation (via conventional breakdown) of a “hot”, self-propagating lightning channel.

2.1 Conventional Breakdown

According to the conventional breakdown mechanism, lightning is initiated via the emission of positive corona from the surface of precipitation particles, highly deformed by strong electric fields in the case of raindrops, coupled with some mechanism whereby the electric field is locally enhanced to support the propagation of corona streamers. Positive streamers are much more likely to initiate lightning than negative ones because they can propagate in substantially lower fields. The most detailed hypothetical scenario of lightning initiation via conventional breakdown is described by Griffiths and Phelps (1976b) who consider a system of positive streamers developing from a point on a hydrometeor where the electric field exceeds the corona onset value of $2.5\text{--}9.5 \times 10^5$ V/m ($2.5\text{--}9.5$ kV/cm). The developing streamers are assumed to form a conical volume that grows longitudinally. The ambient electric field in the thundercloud required to support the propagation of corona streamers, E_0 , was found by Griffiths and Phelps (1976a) from laboratory experiments to be 1.5×10^5 V/m (1.5 kV/cm) at about 6.5 km and 2.5×10^5 V/m (2.5 kV/cm) at about 3.5 km. If the ambient electric field is higher than E_0 , the streamer system will intensify, carrying an increasing amount of positive charge on the propagating base of the cone, which simulates the positive streamer tips, and depositing an equally increasing

amount of negative charge in the conical volume which represents the trails of the positive streamers. As a result, an asymmetric conical dipole is formed, which presumably can serve to enhance the existing electric field at the cone apex representing the origin of the positive streamers on the surface of the hydrometeor. Further, Griffiths and Phelps (1976b) suggest that several conical streamer systems may develop sequentially, each one passing into the debris of its predecessors, to achieve the field enhancement required for breakdown. For representative values of ambient electric field and E_0 at 6.5-km altitude, they report that a series of three to seven such systems can give rise to local enhancement of the ambient electric field up to 1.5×10^6 V/m (15 kV/cm) over a distance of a few meters, which is sufficient to ensure dielectric breakdown and, perhaps, eventually lead to the formation of the stepped leader. The number of passages required to achieve a certain field value depends on the assumed value of the potential of the streamer tip. Griffiths and Phelps (1976b) used a value of 10 kV, based on the results of laboratory experiments reported by Phelps (1974), for most of their calculations. These calculations involve an extrapolation from the relatively small (up to 1 m) gaps used in laboratory experiments to the relatively large distances (of the order of 100 m) over which streamers might travel in a thundercloud.

Loeb (1966) considered a parcel of air containing positively charged raindrops that is swept in the updraft toward the negative charge center to yield positive corona streamers from the raindrops. In this scenario, formation of positive streamers is facilitated by updraft reducing the separation between the oppositely charged regions in the cloud.

Nguyen and Michnowski (1996) considered the effects of many closely spaced hydrometeors in lightning initiation. Their hypothetical mechanism involves a bidirectional streamer development assisted by a chain of precipitation particles, as opposed to the scenario that invokes the propagation of positive streamers alone.

2.2 Runaway Breakdown

Gurevich et al. (1992, 1999) suggested that runaway electrons may play an important role in lightning initiation. In order to “run away”, an electron must gain more energy from the electric field between collisions with air particles than it loses in a collision. The so-called breakeven electric field, which must be exceeded for runaway to occur, depends on altitude. This field decreases exponentially with altitude due to exponential decrease in the air molecule density. At altitudes of 4–6 km, the breakeven electric field is 1.0×10^5 – 1.5×10^5 V/m (1–1.5 kV/cm) (Gurevich et al. 2003), which is about an order of magnitude lower than the conventional breakdown field at these altitudes. The runaway breakdown requires the presence of initial electrons with energies exceeding 0.1–1 MeV. Such energetic electrons are produced in thunderclouds via collisions of very high-energy (10^{15} – 10^{16} eV or greater) cosmic ray particles with atmospheric nuclei. The flux of particles with energies $\geq 10^{16}$ eV is about 0.1 per km^2 per second (Eidelman et al. 2004, Ch. 24). So, for a thundercloud area of about 100 km^2 , they may occur every 100 ms. The initial energetic electrons are sometimes referred to as cosmic ray secondaries. Each very high-energy cosmic ray particle produces 10^6 – 10^7 secondaries (Gurevich and Zybin 2001) in a process that is referred to as the “extensive air shower” (the term used in the cosmic ray physics for “cosmic ray shower”). [Solomon et al. (2001, 2002) additionally considered the high-energy decay products emitted from atmospheric radio nuclides as a source of high-energy electrons.]

If the energetic electrons find themselves in a thundercloud region in which the electric field is greater than the local breakeven field (about 10^5 V/m at an altitude of 6 km), they

can run away. Furthermore, if the high field region extends over a sufficient distance (of the order of a kilometer), an avalanche of runaway electrons and a very large number of relatively slow (a few eV to 100 keV or so) electrons can be produced. If the density of slow electrons reaches a critical value in some small region, the electrical conductivity in that region becomes high enough (of the order of 10^{-4} S/m; Solomon et al. 2001) to form an elongated plasma patch. This elongated (about 10 m long; Solomon et al. 2001) conductor, formed and polarized within microseconds (Gurevich and Zybin 2001), can enhance the electric field near its extremities to the values required for conventional breakdown via avalanches of low-energy (less than 30 eV) electrons. There has been a recent debate on whether a sufficient number of slow electrons can be produced to allow the creation of a plasma patch with conductivity of the order of 10^{-4} S/m (Dwyer and Babich 2011, 2012; Gurevich et al. 2012). Note that the runaway breakdown initiated by an energetic cosmic ray particle (the initial energetic electron is supplied by an external source) is referred to as relativistic runaway breakdown, as opposed to the so-called cold runaway breakdown discussed in Section 8.

According to Gurevich et al. (2003), the formation of a field-enhancing ionized region (“lightning seed”) by a cosmic ray particle with an energy of 10^{16} eV via the runaway breakdown mechanism is associated with a current pulse having an amplitude of 100–200 A. This current pulse is predicted to generate a bipolar electric field pulse with a characteristic full width of 0.2–0.4 μ s (Gurevich et al. 2002). Gurevich et al. (2003) presented submicrosecond-full-width electric field pulses measured at the Tien–Shan Mountain Cosmic Ray station at distances of 5–20 km from lightning discharges that they interpreted as indicative of strong current pulses associated with the formation of the “lightning seed”. Note that these “lightning initiation pulses” are more than an order of magnitude shorter than the shortest initial-breakdown pulses, including the narrow bipolar pulses that have characteristic full widths of a few tens of microseconds (see Sect. 3).

Rakov (2006) presented submicrosecond-scale electric field pulses measured in Florida (at sea level) that are similar to the “lightning initiation pulses” predicted and observed at a high-elevation station by Gurevich et al. (2002, 2003). However, these submicrosecond-scale pulses occurred both before and after the first ordinary (typically tens-of-microseconds-width) initial-breakdown pulse of the lightning flash. It is not clear how the occurrence of multiple submicrosecond-scale pulses can be related to the runaway breakdown lightning initiation mechanism proposed by Gurevich et al. (1999, 2002).

2.3 Lower Positive Charge in the Cloud and Lightning Type

Initiation of the first, stepped leader of a cloud-to-ground flash is thought to be preceded by the so-called preliminary breakdown (PB) which can produce a sequence of characteristic electric field pulses (PB pulse train). The percentage of flashes exhibiting detectable preliminary breakdown pulse trains varies from less than 20 % to 100 % (Nag and Rakov 2009). The largest pulses in the train can exceed in magnitude the following first return-stroke pulse. Nag and Rakov (2009) interpreted the PB pulse train as being generated when a negatively charged channel extends downward from the main negative charge region and encounters an appreciable lower positive charge region (LPCR). In this view, when the LPCR is small, no significant PB pulse train is produced.

While the LPCR may serve to enhance the electric field at the bottom of the negative charge region and thereby facilitate the launching of a negatively charged leader toward ground, the presence of excessive LPCR may prevent the occurrence of negative cloud-to-ground flashes by “blocking” the progression of descending negative leader from reaching

ground (Nag and Rakov 2008). Nag and Rakov (2009) inferred four conceptual lightning scenarios that may arise depending upon the magnitude of the LPCR, illustrated in Fig. 3.

When the magnitude of LPCR is abnormally large, say, comparable in magnitude to that of the main negative charge, as shown in Fig. 3a (left), the so-called inverted intracloud (IC) discharges are expected to occur. In this scenario, a descending negative leader would likely change its direction of propagation to predominantly horizontal, interact with the LPCR, and be unable to forge its way to ground. The result is an inverted IC flash. An example of expected electric field signature of such a discharge is shown in Fig. 3a (right), which exhibits a PB pulse train followed by static field change some tens of milliseconds in duration, indicative of an inverted IC flash (attempted cloud-to-ground leader (Nag and Rakov 2008)). If the lightning channel emerges from the cloud, it can be viewed as an “air discharge” or even as a “spider” lightning, if it develops over a large distance near the cloud base.

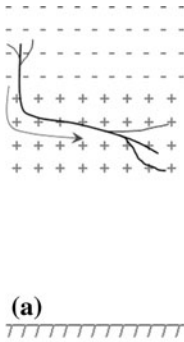
Figure 3b (left) shows the scenario where the magnitude of the LPCR is somewhat smaller than in scenario (a). Similar to scenario (a), a negatively charged leader channel extending vertically from the main negative charge region would become predominantly horizontal, but would eventually make termination on ground. In this case, the discharge can be viewed as a hybrid flash (an IC followed by a cloud-to-ground (CG) discharge). The electric field signature expected for this type of discharge is shown in Fig. 3b (right), which shows a PB pulse train followed by a field change characteristic of a cloud discharge lasting for about 50 ms, followed by the first return-stroke waveform of a CG flash.

If the magnitude of the lower positive charge relative to the main negative charge is even smaller, as shown in Fig. 3c (left), the descending negative leader would traverse the positive charge region and continue to propagate in a predominantly vertical direction to ground. The electric field signature expected to be produced in this case is shown in Fig. 3c (right). It exhibits a PB pulse train and stepped-leader waveform followed by the first return-stroke (RS) waveform. Leader duration, found as the time interval between PB and RS, is about 20 ms.

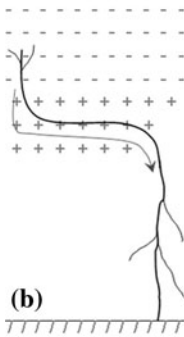
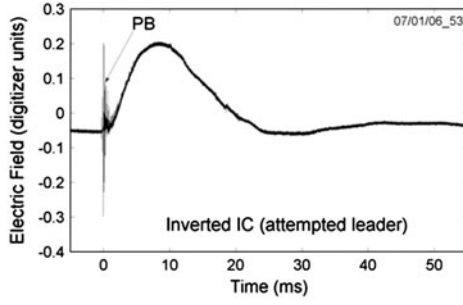
Figure 3d (left) shows the scenario when the LPCR is insignificant. This scenario is similar to scenario (c), except for the LPCR playing essentially no role in negative-leader initiation. The electric field signature produced in this case is expected to be that of a stepped-leader/return-stroke sequence not preceded by a detectable PB pulse train, as shown in Fig. 3d (right).

3 Compact Intracloud Lightning Discharges

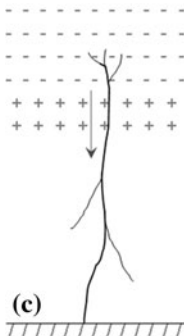
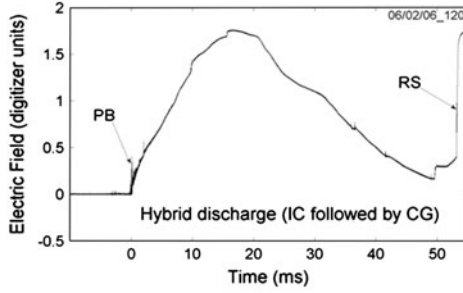
There is a special type of lightning that is thought to be the most intense natural producer of HF-VHF (3–300 MHz) radiation on Earth. It is referred to as Compact Intracloud Discharge (CID). CIDs received their name due to their relatively small (hundreds of meters) spatial extent. They tend to occur at high altitudes (mostly above 10 km), appear to be associated with strong convection (however, even the strongest convection does not always produce CIDs), tend to produce less light than other types of lightning discharges, and produce single VLF-LF electric field pulses (Narrow Bipolar Pulses or NBPs) having typical full widths of 10–30 μ s and amplitudes of the order of 10 V/m at 100 km, which is comparable to or higher than for return strokes in cloud-to-ground flashes. As an illustration of their VLF-LF intensity, 48 CIDs examined in detail by Nag et al. (2010) were recorded by 4–22 (11 on average) stations of the U.S. National Lightning Detection Network (NLDN), whose average baseline is 300–350 km. According to Nag et al. (2010),



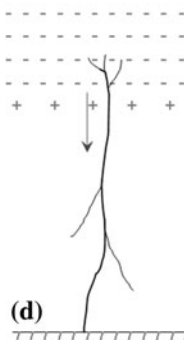
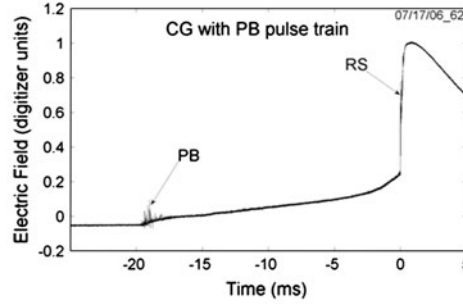
(a)



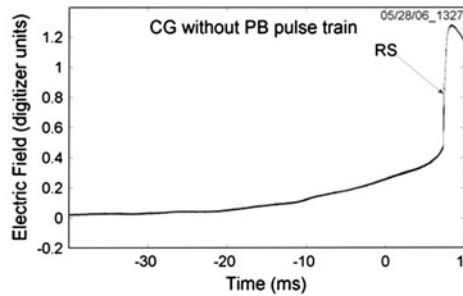
(b)



(c)



(d)



◀ **Fig. 3** The left panels schematically show four types of lightning that may arise depending upon the magnitude of the LPCR. The charge configuration in each of the scenarios represents only its vertical profile (no lateral boundaries are shown). *Arrows* indicate the direction of propagation of negative leader. The corresponding examples of expected electric field signatures are shown in the *right panel*. The field waveforms are from four different thunderstorms recorded at some tens of kilometers at the Lightning Observatory in Gainesville (LOG), Florida, using the same instrumentation with a decay time constant of 10 ms. *PB* preliminary breakdown pulse train, *RS* return-stroke waveform. Adapted from Nag and Rakov (2009)

the majority (about 73 %) of CIDs appeared to occur in isolation from any other lightning process (within the length of the record, which was 500 ms with a 100-ms pre-trigger), while about 24 % were found to occur prior to, during, or following cloud-to-ground or “normal” cloud lightning. About 18 % were associated with cloud flashes and 6 % with ground ones. About 4 % of CIDs were isolated from “normal” lightning, but occurred in pairs with separation times of some tens to a few hundreds of milliseconds. An example of CID occurring prior to a cloud-to-ground discharge is shown in Fig. 4. The top and bottom panels show correlated wideband electric field and VHF radiation records, respectively, both displayed on a 170-ms time scale. In the top panel, PB stands for the preliminary breakdown, and two return-stroke signatures are labeled RS1 and RS2. Note that, while the CID and return-stroke signatures are comparable in magnitude in the top panel, the amplitude of the VHF signature of CID is much smaller than those of other lightning processes (PB, RS1, and RS2) seen in the bottom panel. It is possible that the CID played a role in facilitating the PB that resulted in the cloud-to-ground discharge.

Various electromagnetic signatures of a CID on a microsecond time scale are shown in Fig. 5. Perhaps the most puzzling feature of these mysterious lightning events is the fact that their VHF radiation (which is indicative of PB and leader processes creating a new lightning channel), and their wideband signature (which is indicative of a current wave propagating along an already existing channel) appear to be generated at the same time, as seen in Fig. 5d where those signatures are superimposed.

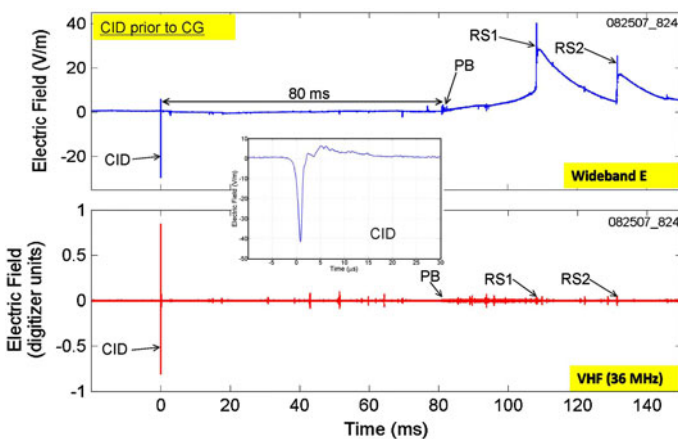


Fig. 4 Electric field and VHF (36 MHz) radiation from a CID that was followed (80 ms later) by the preliminary breakdown of a multiple-stroke cloud-to-ground (CG) discharge. Inset shows the CID signature on an expanded (5 μ s per division) timescale. The signals were recorded at the Lightning Observatory in Gainesville (LOG), Florida

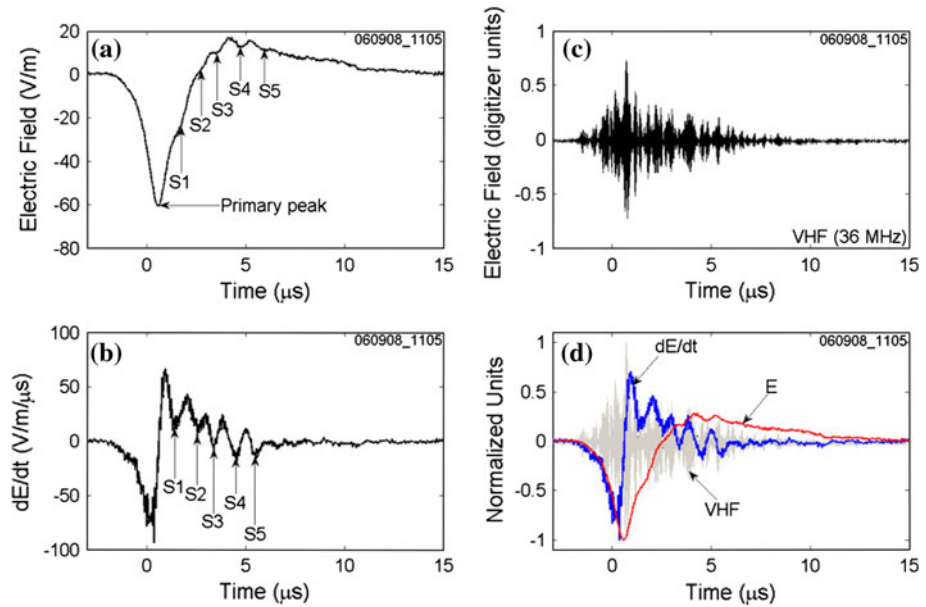


Fig. 5 **a** Wideband (16 Hz–10 MHz) vertical electric field, **b** dE/dt , and **c** VHF radiation signatures of a CID recorded at the Lightning Observatory in Gainesville (LOG), Florida. It occurred at an unknown distance and transferred negative charge downward. The three signatures are overlaid in **(d)** for direct comparison. S1–S5 are five secondary peaks appearing as pronounced oscillations in **(b)** and mostly as shoulders in **(a)**. These secondary peaks are indicative of multiple reflections from the radiating-channel ends. Adapted from Nag and Rakov (2010a)

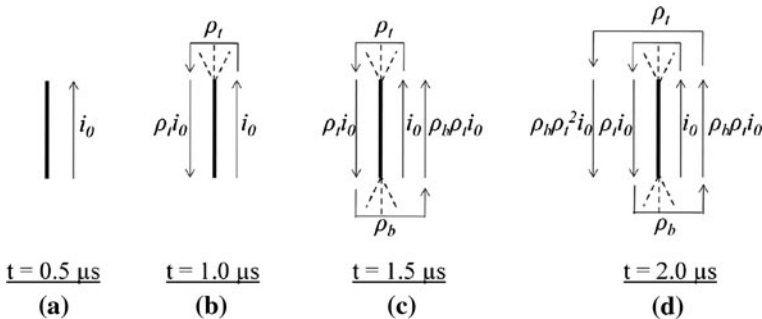


Fig. 6 Schematic representation of the bouncing-wave mechanism of CID for the case of channel length $\Delta h = 100$ m and propagation speed $v = 2 \times 10^8$ m/s. Current-wave duration is much longer than the channel traversal time. *Straight arrows* represent current waves on CID channel, and *bracket-shaped arrows* represent the process of wave reflection at the ends. If $\rho_b = \rho_t = 1$ (short-circuit conditions), it is the same wave bouncing between the ends (folding on itself). If $\rho_b = \rho_t = -1$ (open-circuit conditions), the wave changes polarity each time it hits the end. If $\rho_b = \rho_t = -0.5$, the current wave changes polarity and is reduced in magnitude by a factor of 2 at each end. If $\rho_t = 0$, the wave is fully absorbed at the *top end*. For $|\rho_t| < 1$ and $|\rho_b| < 1$, partial absorption takes place at the *top* and *bottom*, respectively. It is expected that reflected current waves will reduce current at each end, while corresponding voltage will be enhanced there. As a result, corona-like electrical breakdown (shown by *dashed lines*) may occur at the channel ends. Breakdown associated with the incident wave, i_0 , is not shown here

As seen in Fig. 5, there is evidence of reflections (five secondary peaks labeled S1 to S5) in the wideband electric field and particularly dE/dt signatures, although generally they may be undetectable in measured field waveforms. On the basis of the experimental evidence of multiple reflections and modeling, Nag and Rakov (2010a) inferred that, from the electromagnetic point of view, the CID is essentially a bouncing-wave phenomenon. Some tens of reflections may occur at both radiating-channel ends, possibly serving to maintain channel conductivity. The process can be viewed as a long wave repeatedly folding on itself, as schematically shown in Fig. 6, so that the electromagnetic signature duration is not necessarily a measure of radiator length.

Because of relatively short channel length, relatively long current waveform, and relatively high propagation speed, the current distribution along the CID channel is often not much different from uniform, expected for a Hertzian (electrically short) dipole. For the Hertzian dipole approximation and estimated (from reflection signatures) or assumed radiator length, a number of electrical parameters can be readily found from measured wideband electric field waveforms. Nag and Rakov (2010b) inferred for 48 CIDs that geometric mean (GM) values of peak current, zero-to-peak current risetime, and charge transfer in the first 5 μs are 64 kA, 4.9 μs , and 142 mC, respectively. They also estimated the GM peak radiated power and energy radiated in the first 5 μs to be 28 GW and 32 kJ, respectively. CID peak currents are comparable to or higher than those for first return strokes in cloud-to-ground lightning, while their peak radiated (wideband) power is about a factor of 2 larger than that for first return strokes and an order of magnitude larger than for subsequent return strokes.

CIDs appear to be capable of altering the course of lightning discharge activity on an individual flash scale (Nag et al. 2010) and, hence, can be contributing to production of gigantic jets. Krehbiel et al. (2008) reported a CID that occurred 800 ms prior to a gigantic jet. Also, Lu et al. (2011) reported on two gigantic jets, one in Florida and one in Oklahoma, that were each preceded by an ordinary cloud flash apparently initiated by a CID, the latter occurring about 300 and 500 ms prior to the initiation of gigantic jet, respectively.

4 Negative-Leader Stepping Process

The step-formation process in lightning occurs on a time scale of less than 1 μs or so. As a result, it has never been resolved in optical records. On the other hand, there appears to be a qualitative similarity between the lightning negative stepped leader and the negative stepped leader of the long laboratory spark. The latter type of leader is much better studied via the use of electronic image-converter cameras in conjunction with the measurement of current through the air gap. The negative long spark leader exhibits distinct steps when the gap length is several meters or more. Gorin et al. (1976), for example, reported that a 6-m rod-plane gap was bridged by a negative leader in 3–5 steps. It is worth noting that stepping is observed in lightning negative leaders regardless of whether they are initiated in the cloud (downward leaders) or at the grounded object (upward leaders). This fact suggests that the mechanism of formation of a step is determined primarily by the processes at the leader tip and in the leader channel rather than being determined by the source (cloud charge for lightning and impulse generator circuitry for long laboratory sparks).

The development of the negative stepped leader in a long laboratory spark, based on a description given by Gorin et al. (1976), is illustrated in Fig. 7 which schematically shows a snap-shot (left) and a time-resolved optical picture (upper right) including an initial impulsive corona from the negative high-voltage electrode and the first two steps, along

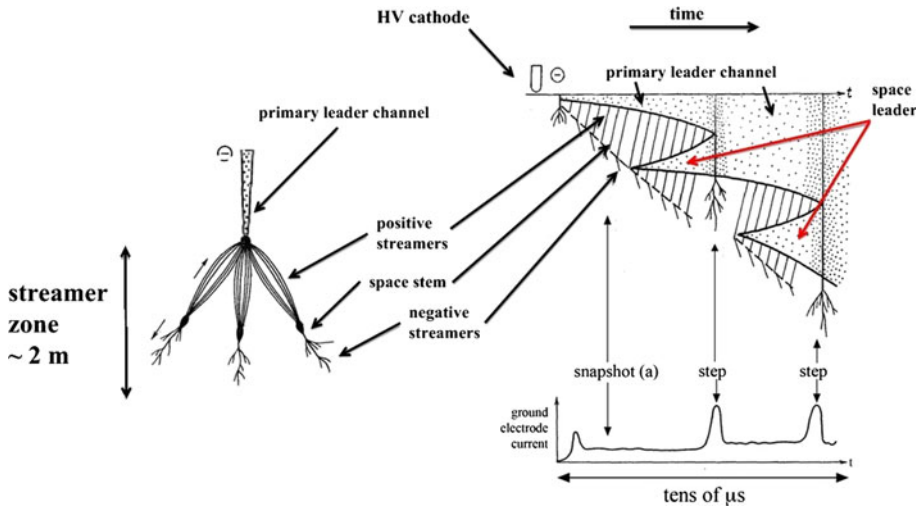


Fig. 7 Illustration of the development of negative stepped leader in a long laboratory spark, based on a description given by Gorin et al. (1976). It schematically shows a snap-shot (left) and a time-resolved optical picture (upper right) including an initial impulsive corona from the negative high-voltage electrode and the first two steps, along with the corresponding current through the gap (lower right). Adapted from Biagi et al. (2010)

with the corresponding current through the gap (lower right). The snap-shot shows the primary leader channel and three streamer branches that appear to be extending from the leader tip. Each streamer branch has a plasma formation, termed space stem, and positive (upward-directed) and negative (downward-directed) streamers. The initial impulsive corona, a system of branched filamentary channels seen in the time-resolved picture, serves to heat the air near the high-voltage electrode and to form the initial section of the leader plasma channel. This process produces the first pulse in the current record (lower right), the other two current pulses being associated with the two leader steps. The initial section of the leader channel extends from the high-voltage electrode into the gap. The leader tip is brighter than the channel behind it and is shown as a slightly curved, negatively sloped solid line. The positive streamers develop toward the leader tip (these are shown in the time-resolved picture by longer, positively sloped solid lines), and the negative streamers develop into the gap (these are shown by shorter, negatively sloped solid lines). The oppositely charged streamers start from the space stem (shown as a negatively sloped dashed line), which moves into the gap in front of the leader tip. The air behind the moving space stem apparently remains essentially an insulator. It is presently unknown how a space stem is formed ahead of the leader tip (Bazelyan and Raizer 2000). When the space stem is sufficiently heated, it gives rise to, in effect, a section of the leader channel that is not connected to either of the electrodes and extends in both upward and downward directions. The bidirectional channel extension is shown in Fig. 7 (upper right) as a pair of slightly curved and diverging solid lines drawn from a common origin on the slanted dashed line. This unconnected (space) channel, sort of a “bidirectional leader,” was termed a secondary channel by Bazelyan et al. (1978) and a space leader by Larigaldie et al. (1992). The upward-extending part of this “bidirectional leader” is charged positively, and the downward-extending part is charged negatively.

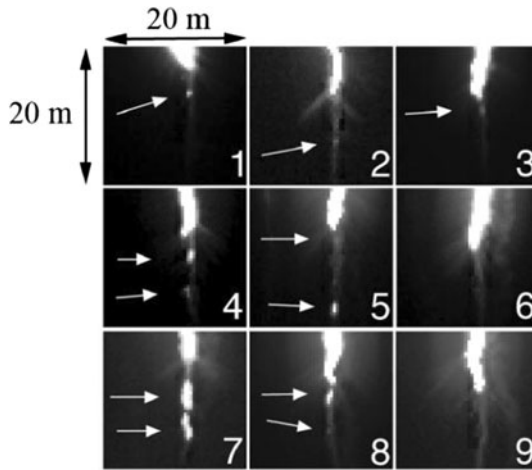


Fig. 8 The bottom 20 m of the downward-extending leader channel of a triggered-lightning flash (Camp Blanding, Florida) in the nine high-speed video frames (240 kfps, $4.17 \mu\text{s}$ per frame). Each image shows about $20 \text{ m} \times 20 \text{ m}$. The white arrows point to the luminous segments (space stems or leaders), 1–4 m in length, that formed separately from and 1–10 m below the downward-extending leader channel. The leader traveled about 100 m from frame 1 to frame 9 where it was about 30 m above its termination point. The return stroke began during frame 10. Adapted from Biagi et al. (2010)

The first leader step is formed at the instant when the upward-moving positive end of the space-leader channel makes contact with the downward-moving negative tip of the primary (that is, connected to the high-voltage electrode) leader channel. At that moment, the very high potential (close to the potential of the high-voltage electrode) of the primary leader channel is rapidly transferred to the lower end of the secondary (space-leader) channel. As a result, a burst of negative streamers (thought to be responsible for production of X-rays by negative leaders; see Sect. 8) is produced at the bottom of the newly added channel section. Such a breakdown generates a current pulse which propagates toward the high-voltage electrode and briefly illuminates the entire channel. Thus, in the negative leader, the occurrence of each luminous step is caused by the connection of a secondary channel (space leader) to the primary leader channel. The development of the next step of a negative leader begins with the formation of a new space stem ahead of the newly added leader step.

Biagi et al. (2010), using a high-speed video camera ($4.17\text{-}\mu\text{s}$ frame integration time), imaged the bottom 150 m of a downward negative, dart-stepped leader in a rocket-and-wire triggered flash. They observed vertically elongated luminous formations, 1–4 m in length, that were separated by darker gaps, 1–10 m in length, from the bottom of the downward-extending leader channel, illustrated in Fig. 8. These formations, indicated by white arrows in seven of the nine frames shown in Fig. 8, are similar to the space stems or space leaders that have been imaged in long negative laboratory sparks. It is worth noting that the frame integration time (about $4 \mu\text{s}$) was longer than the duration of step-formation process (less than $1 \mu\text{s}$), so that individual steps could not be resolved. Similar observations for downward negative stepped leaders in natural lightning were reported by Hill et al. (2011).

Wang et al. (1999b), using a high-speed (100-ns sampling interval) digital optical imaging system (ALPS) in rocket-triggered lightning experiments at Camp Blanding,

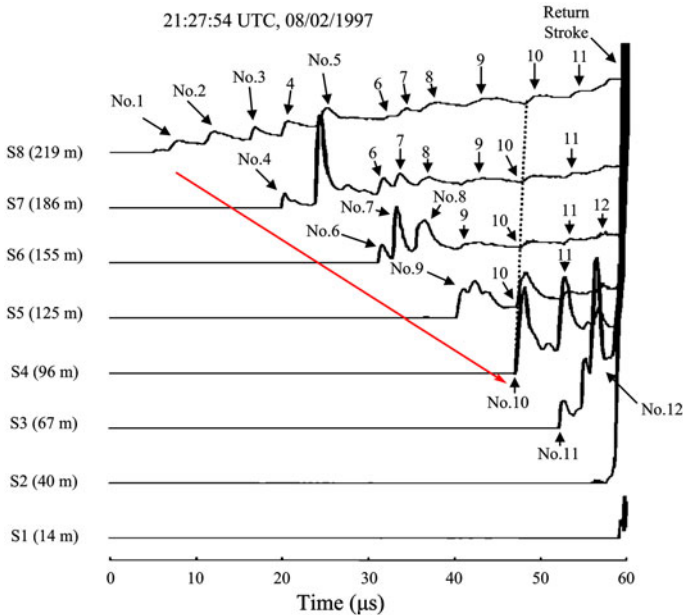


Fig. 9 Light versus time waveforms at different heights above ground for a dart-stepped leader in a negative flash triggered using the rocket-and-wire technique at Camp Blanding, Florida. *Large red, negatively sloped arrow* indicates the overall downward progression of the leader. Light pulses associated with individual steps are numbered. They appear to originate at the tip of the downward-extending leader channel and propagate upward. Adapted from Wang et al. (1999b)

Florida, reported observations of luminosity waves that originated at newly formed leader steps in a dart-stepped leader and propagated toward the cloud, as illustrated in Fig. 9. Shown in this Figure are leader light versus time waveforms at eight different heights above ground. The overall downward progression of the leader is shown by large red, negatively sloped arrow. The light pulses corresponding to individual steps are numbered. These pulses appear to move upward, as indicated by dotted, positively sloped line for pulse No. 10, and attenuate to about 10 % of the original luminosity value after traveling 50 m or so. The dotted line is considerably steeper than the large red arrow, which means that the upward light pulse speed (mean = 6.7×10^7 m/s) is much higher than the downward leader progression speed (2.5×10^6 m/s, on average). Note that the spatial resolution of ALPS was about 30 m and, because of that, not all the individual step pulses were resolved (more than one step could be formed within 30 m).

Observations of step-generated upward-moving luminosity waves for downward negative stepped leaders in natural lightning were reported by Chen et al. (1999) and Hill et al. (2011).

5 Lightning Attachment Process

The process of lightning leader attachment to ground or to a grounded object is one of the least understood and poorly documented processes of the cloud-to-ground lightning discharge. It is generally assumed that the attachment process begins when an upward-moving

leader is initiated in response to the approaching downward-moving leader at the ground or, more likely, at the tip of an object protruding above ground. It is possible that two or more upward leaders are launched from the ground toward the descending leader, perhaps in response to different branches of the descending leader. An upward leader that makes contact with a branch of a downward leader is called an upward connecting leader. The so-called break-through phase, is assumed to begin when the relatively low conductivity streamer zones ahead of the two propagating leader tips meet to form a common streamer zone. The subsequent accelerated extension of the two relatively high conductivity plasma channels toward each other takes place inside the common streamer zone. The break-through phase can be viewed as a switch-closing operation that serves to launch two return-stroke waves from the point of junction between the two plasma channels. One wave moves downward, toward the ground, and the other upward, toward the cloud. The downward-moving return-stroke wave quickly reaches the ground, and the resultant upward reflected wave from ground catches up with the upward-moving return-stroke wave from the junction point. The latter is the case because the reflected wave from the ground propagates in the return-stroke-conditioned channel and, hence, is likely to move faster than the upward wave from the junction point that propagates along the leader-conditioned channel (Rakov 1998). When the waves bouncing between the ends of the growing return-stroke channel decay, a single upward-moving wave is formed. Thus, the lightning attachment process involves two plasma channels growing toward each other, initially in air (the upward connecting leader phase) and then inside the streamer zone (the break-through phase). It is a matter of definition whether the very short-lived bidirectional return-stroke wave should be considered a part of the attachment process or a part of the return stroke.

Wang et al. (1999a), using the digital optical imaging system ALPS with 3.6-m spatial and 100-ns time resolution, observed an upward connecting leader in one triggered-lightning stroke and inferred the existence of such a leader in another one. A sketch of the time-resolved image for the former event is shown in Fig. 10, in which the break-through phase is completed at $t = 0$. In both events, the return stroke was initially a bidirectional process that involved both upward- and downward-moving waves which originated at 7–11 m (in the event with the imaged upward connecting leader) and 4–7 m (in the event

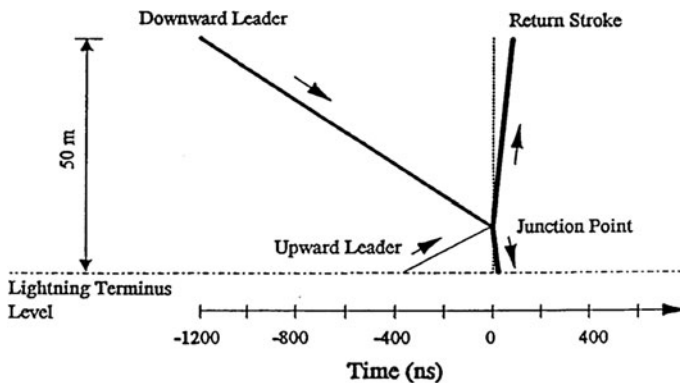


Fig. 10 Schematic representation of the first optical images of upward connecting leader and bidirectional return-stroke process in rocket-triggered lightning (Camp Blanding, Florida). Adapted from Wang et al. (1999a)

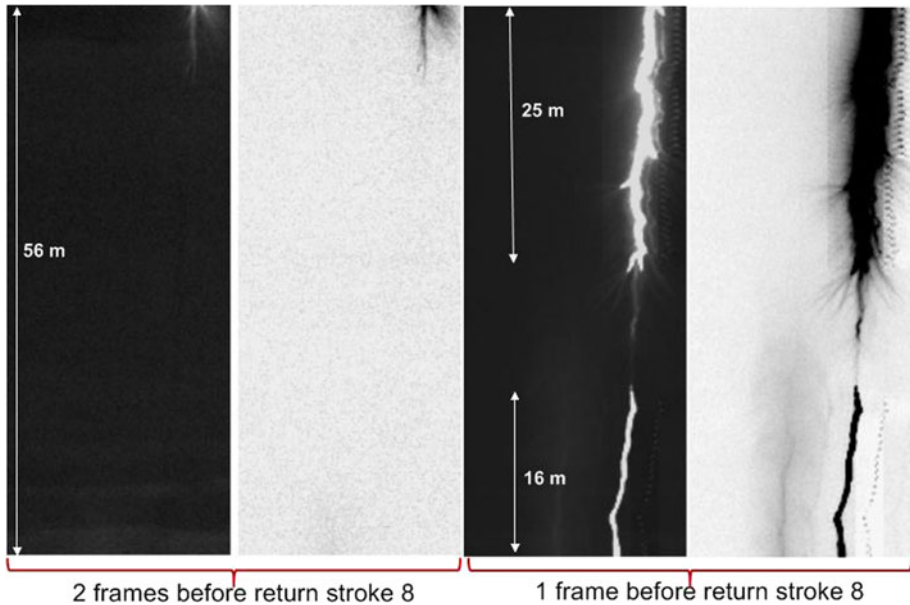


Fig. 11 Two frames of high-speed video record (20- μ s frame integration time) showing a dart-stepped leader and attachment process in a negative lightning flash triggered using the rocket-and-wire technique at Camp Blanding, Florida. Each frame is shown as a positive and a negative. Both upward connecting leader (16-m long) and break-through phase are seen in the second frame (two rightmost images). Adapted from Biagi et al. (2009)

with no imaged upward connecting leader). The imaged upward connecting leader had a light intensity one order of magnitude lower than its associated downward dart leader. The propagation speed of the upward connecting leader was estimated to be about 2×10^7 m/s, similar to the typical speed of downward dart leaders.

Biagi et al. (2009), using a high-speed video camera (20- μ s frame integration time), recorded upward connecting leaders, ranging from 9 to 22 m in length, in eight strokes of a single rocket-triggered lightning flash. One of these upward leaders, whose length was 16 m, is shown in Fig. 11 (see panels labeled “1 frame before return-stroke 8”). This Figure also shows a faint streamer filament between the downward and upward connecting leaders, apparently indicative of the beginning of the break-through phase. Similar features can be seen in optical images of four 4.5-m negative laboratory sparks at different stages of their development, shown in Fig. 12. Only downward leader is seen in Fig. 12a, while both downward and upward leaders are present in Fig. 12b–d. In Fig. 12b, L is the length of just-formed step with a pronounced burst of negative streamers from its lower end. Remnants of such a burst are also seen in Fig. 12c. The streamer burst signifies the final stage of step-formation process (see Sect. 4) and is thought to be the source of X-rays produced by negative leaders (see Sect. 8). In Fig. 12b, there is a faint streamer filament bridging the gap between the downward and upward leaders, similar to that seen in Fig. 11. There is also faint luminosity between the downward and upward leaders in Fig. 12d, while in the spark shown in Fig. 12c, connection between the two leader channels is already established.

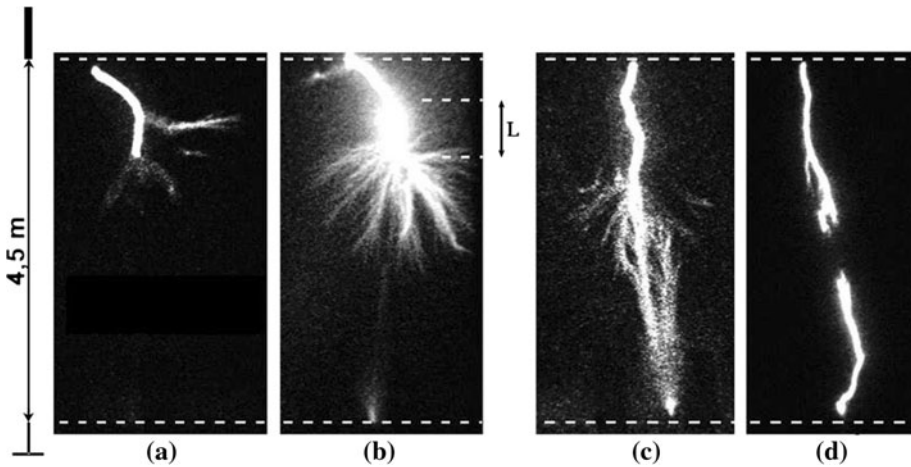


Fig. 12 Single-frame image-converter-camera records of four negative laboratory discharges in a 4.5-m rod-rod gap. The high-voltage (*top*) electrode is negative (an impulse with a peak of -2.2 MV, time to peak of 130 μ s, and time to half-peak value on the tail of $7,500$ μ s was applied). Frame duration in **a**, **b**, and **c** is 2 μ s, and in **d**, it is 0.5 μ s. Only downward leader is seen in **a**. Upward connecting leaders and break-through phase are seen in **b**, **c**, and **d**. *L* in **b** is the length of just-formed step (note the burst of negative streamers from the lower end of the step). Adapted from Lebedev et al. (2007)

6 Lightning M-Component Mechanism

M components are perturbations (or surges) in the relatively steady continuing current and in the associated channel luminosity. The M in the term M component stands for D.J. Malan who was the first to study this lightning process. “Classical” M-components occur in a single channel to ground, whose length is of the order of a kilometer or more. They are apparently excited at the upper extremity of the channel (in the cloud) by either recoil leaders or via the interception of separate in-cloud leaders by a grounded current-carrying channel (Yoshida et al. 2012). Similar to leader/return sequences and to continuing currents, M components serve to transport negative electric charge from the cloud to ground. M-components are likely to occur also during the initial stage of object-initiated and rocket-triggered lightning. The M-component mode of charge transfer to ground differs from the dart-leader/return-stroke mode in that the former requires the presence of a current-carrying channel to ground, while the latter apparently occurs along the remnants of the previously formed channel when there is essentially no current flowing to ground. These two modes of charge transfer to ground, as well as the continuing current mode, are discussed by Rakov and Uman (2003, Fig. 1.2).

From a comparison of the electric fields 30 m from the triggered-lightning channel and the corresponding channel-base currents of M-components in conjunction with modeling, Rakov et al. (1995) have proposed a two-wave mechanism for this lightning process. According to this mechanism, an M component is essentially a guided-wave process that involves a downward progressing incident wave (the analog of a leader) and an upward progressing wave that is a reflection of the incident wave from the ground (the analog of a return stroke). Ground is sensed by the incident M-wave as essentially a short circuit, so the reflection coefficient for current at ground is close to $+1$, and the reflection coefficient for the associated charge density is close to -1 . Because the reflection coefficients for the

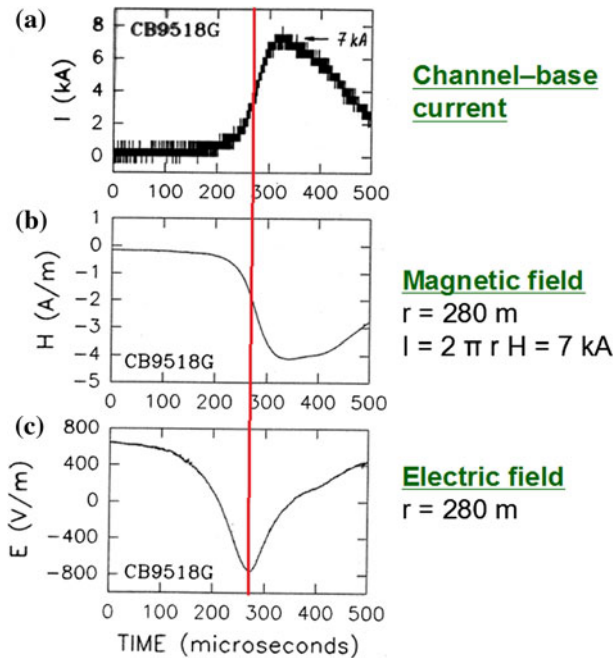


Fig. 13 **a** Channel-base current, **b** magnetic field, and **c** electric field for a large M-component that followed the second stroke of a rocket-triggered lightning flash at Camp Blanding, Florida. The fields were recorded at a distance of 280 m from the lightning channel. Red vertical line indicates the position of negative electric field peak. Note that the electric field peak occurs when the channel-base current exceeds 3 kA, which is in contrast with the relationship between close electric field and channel-base current characteristic of leader/return-stroke sequences. Adapted from Rakov et al. (1998)

traveling waves of current and charge density are different, the incident and reflected waves of current (which determine the close magnetic fields) add at each channel section, while the incident and reflected waves of charge density (which determine the close electric fields) subtract. As a result, at close ranges, the M-component magnetic field has an overall waveshape similar to that of the channel-base current, whereas the M-component electric field has a waveform that appears to be the time derivative of the channel-base current. The key point here is that the negative electric field peak occurs when the impulsive channel-base current has already significantly increased relatively to the background continuing current, as illustrated in Figs. 13 and 14. [Note that, in Fig. 14, both the “classical” M-component and an M-component-like process termed “ICC pulse”, which occurred during the initial stage of rocket-triggered lightning, showed essentially the same behavior.] For example, in Fig. 13, the negative electric field peak in (c) occurs when the channel-base current, shown in (a), exceeds 3 kA. Thus, the M-component current pulse at the channel base begins while the bulk of the associated charge is still being transported toward the ground in the upper channel sections, as if the return-stroke-like process was commencing at ground before the arrival of leader-like process there. This is in contrast with the close electric field signature of leader/return-stroke sequences, in which the electric field peak signifies the arrival of descending leader at ground and the onset of resultant return-stroke current there (a significant increase in current at the channel base does not occur until the arrival of leader at ground). The formation of M-component

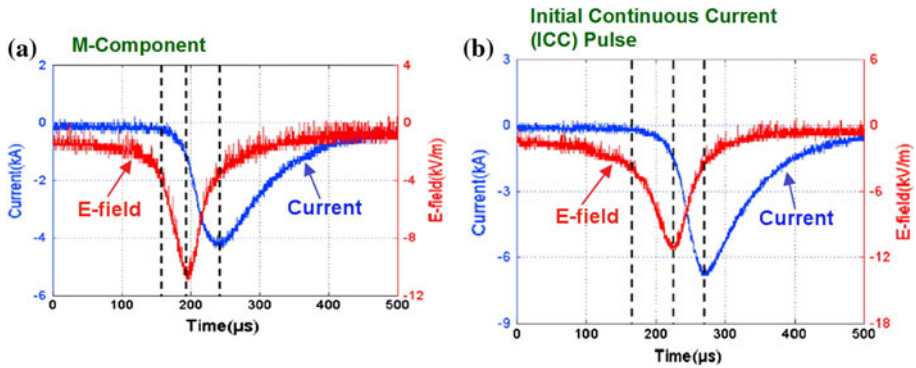


Fig. 14 Waveforms of channel-base current (inverted relative to that in Fig. 13a) and electric field at a distance of 30 m from the lightning channel for **a** an M-component and **b** an ICC pulse in flash 0902 triggered using the rocket-and-wire technique in Shandong, China. The vertical dashed lines indicate the times of (from left to right) the current pulse onset, the electric field peak, and the current pulse peak. Note that in both cases, the current pulse begins well before the electric field peak, the behavior similar to that seen in Fig. 13. Adapted from Qie et al. (2011)

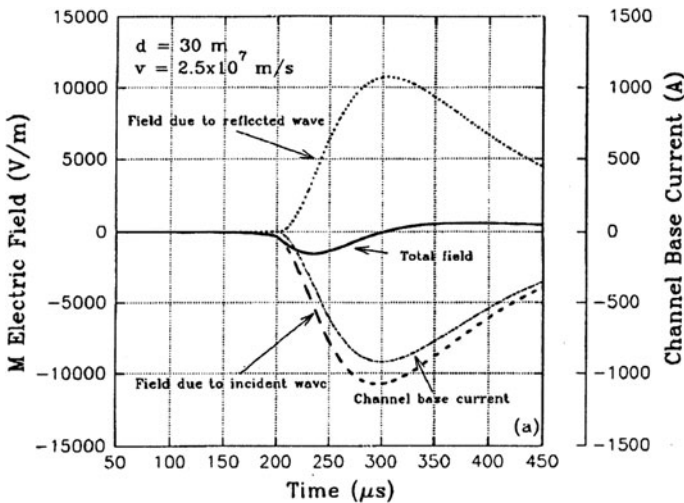


Fig. 15 Formation of M-component electric field waveform (labeled “Total field”) at a distance of 30 m from the lightning channel, computed according to the two-wave mechanism. The total field is the sum of the fields due to incident and reflected M-current waves, the latter fields being shown by *dashed* and *dotted lines*, respectively. Also shown is the corresponding channel-base current (inverted relative to that in Fig. 13a) which begins at $t = 200 \mu\text{s}$, when the incident M-current wave arrived at ground. The incident and reflected M-current waves are assumed to have identical waveforms (perfect reflection at ground) and equal propagation speeds ($2.5 \times 10^7 \text{ m/s}$). Adapted from Rakov et al. (1995)

electric field waveform at 30 m from the lightning channel, computed according to the two-wave mechanism proposed by Rakov et al. (1995), is illustrated in Fig. 15. A good qualitative correspondence with measurements shown in Figs. 13 and 14 is evident. Specifically, the negative total field peak in Fig. 15 occurs when the current has attained a magnitude of a few hundred amperes (an appreciable fraction of its peak).

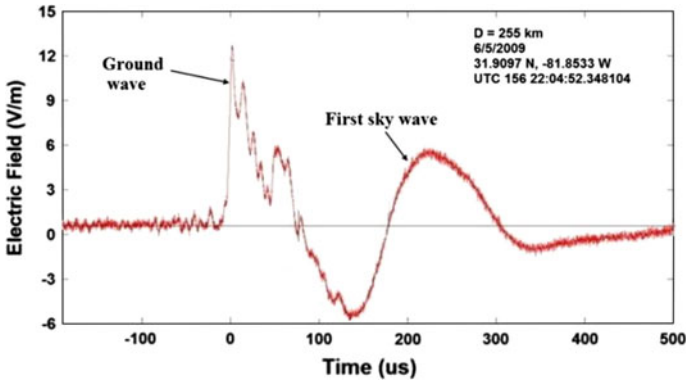


Fig. 16 Vertical electric field waveform of a negative first return stroke at a distance of 255 km, shown on a 700- μ s time scale. The waveform was recorded at the Lightning Observatory in Gainesville (LOG), Florida, at about 18:05 local time. The ground wave (the first positive half-cycle followed by the opposite polarity overshoot) and first sky wave (the second positive half-cycle) are marked. Adapted from Haddad et al. (2012)

M-component type processes in positive lightning may play a role in the initiation of so-called delayed sprites that occur many tens of milliseconds after the return stroke (e.g., Yashunin et al. 2007).

7 Lightning Interaction with the Ionosphere

Haddad et al. (2012) analyzed wideband (16 Hz to at least 10 MHz) vertical electric field waveforms of first and subsequent return strokes in negative natural lightning. At distances ranging from 100 to 330 km, electric field waveforms, recorded primarily under daytime conditions, tended to be oscillatory (see Fig. 16), showing two cycles within 500 μ s, with the corresponding frequency being about 4–5 kHz. The initial positive half-cycle and the following opposite polarity overshoot constitute the ground wave, and the second positive half-cycle is the one-hop ionospheric reflection (first sky wave), as confirmed by FDTD modeling. The observed differences in arrival times of these two waves for subsequent strokes are considerably smaller than for first strokes, suggesting that the first-stroke electromagnetic field caused a descent of the lower ionosphere. For most (103 out of 124) of the subsequent strokes examined by Haddad et al. (2012), the mean reflection height was about 76 km, which is 5 km lower than that for the first strokes, but the height distribution exhibited a long tail, extending to as low as 30 km. Haddad et al. (2012) speculated that there might be cumulative contributions of multiple strokes to lowering the ionospheric reflection height. Waveforms of four strokes in the same flash that apparently illustrate this effect are shown in Fig. 17. In this Figure, ground-wave peaks of all the strokes are aligned, and broken vertical line indicates the position of the first sky-wave peak for the first stroke. Clearly, the separation between the ground and sky waves decreases with increasing stroke order. The corresponding effective ionosphere heights for these four strokes are 93, 90, 86, and 69 km. Note that such a pronounced ionosphere descent is not seen for all flashes, particularly at night.

Lightning-driven mechanisms that are known to perturb the ionosphere are elves expanding over a radial distance of up to a few hundreds of kilometers across the bottom of

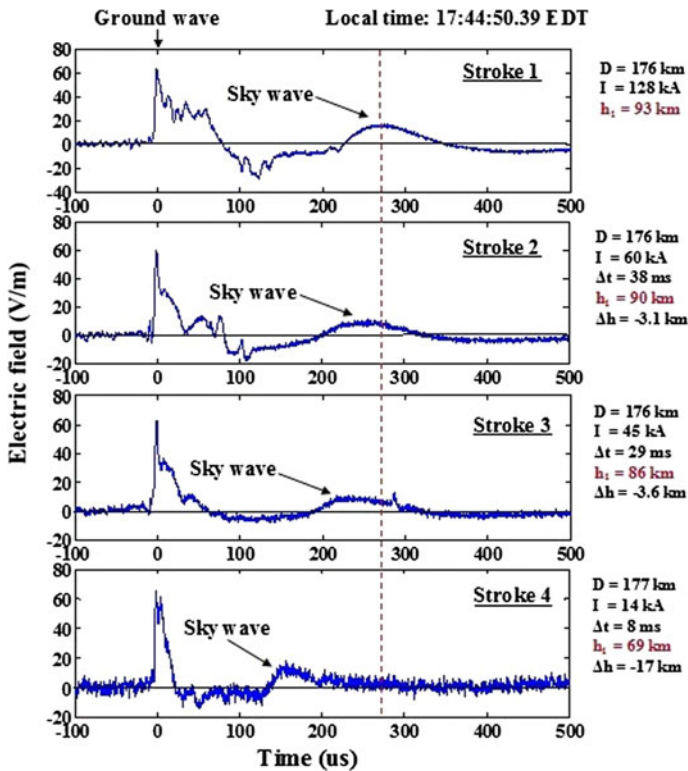


Fig. 17 Vertical electric field waveforms of four negative return strokes in the same flash at a distance of about 176 km, shown on a 600- μ s time scale. The waveforms were recorded at the Lightning Observatory in Gainesville (LOG), Florida, at about 17:45 local time. The ground wave and first sky wave are marked. The vertical broken line indicates the position of the maximum of the first sky wave for stroke 1. Note that the maxima of the first sky waves for strokes 2 through 4 exhibit progressively smaller delays relative to the ground wave maximum, which corresponds to the reduction in the ionospheric reflection height from 93 km for stroke 1 to 90, 86, and 69 km for strokes 2, 3, and 4, respectively. Δt is the preceding interstroke interval, and I is the NLDN-reported peak current. Adapted from Somu et al. (2012)

the ionosphere, halos occurring below elves altitudes and having smaller radial extent, and sprites, extending between 40 and 90 km heights and often having faint tendrils extending from 50 km or so to altitudes as low as 20 km (near the cloud tops). The discharges analyzed by Haddad et al. (2012) were of negative polarity and thus were likely not to have created sprites. Due to their independence of lightning polarity and larger radial extent, elves appear to be the most likely candidate. Lightning interactions with the ionosphere are relatively brief (for example, optical elves typically last less than 1 ms), but their effects can persist for 10–100 s (e.g., Inan et al. 2010), which is much longer than the duration of causative lightning flash.

8 X-ray Production by Cloud-to-Ground Leaders

All types of leaders produce X-ray emissions with individual photon energies typically ranging from 30 to 250 keV (the latter being about twice the energy of a chest X-ray),

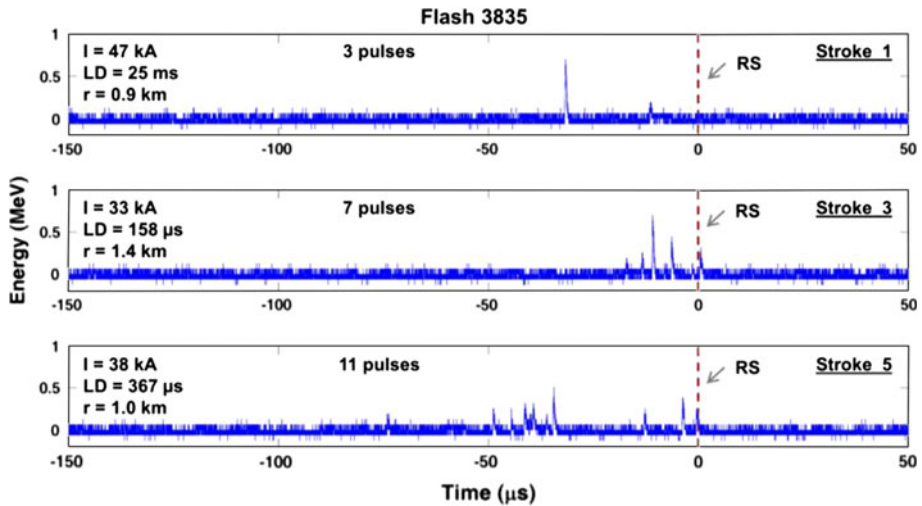


Fig. 18 X-rays produced by stroke 1 (*top*), stroke 3 (*middle*), and stroke 5 (*bottom*) of 11-stroke flash 3835. Strokes 2 and 4 did not produce detectable X-rays. Only the first five strokes of this flash were recorded at LOG. Vertical broken lines labeled RS indicate the position of the return stroke. NLDN-reported distances for strokes 1–5 were 0.9–1.4 km. Judging from leader durations (LD), strokes 3 and 5 each followed a previously formed channel. Some pulses seen in the plots are due to multiple photons arriving within the response time of the X-ray detector, that is, are actually each a superposition (pile-up) of two or more individual pulses. All discernible individual pulses are included in the pulse count given on the plots. Adapted from Mallick et al. (2012)

although occasionally photons in the MeV range were observed. Note that in the lightning literature, the MeV-range photons are often attributed to gamma radiation (e.g., Dwyer et al. 2011). These emissions are associated with the descending leader tip and with the ground attachment process. It is likely that X-ray emissions from cloud-to-ground lightning leaders are associated with the so-called cold runaway (also known as thermal runaway) breakdown, in which very strong electric fields (>30 MV/m) cause the high-energy tail of the bulk free electron population to grow, allowing some electrons to runaway to high energies. Such very high fields may be present at streamer heads or leader tips (Moss et al. 2006; Cooray et al. 2009, 2010).

Mallick et al. (2012) recorded 23 strokes (8 first and 15 subsequent) within 2 km of the Lightning Observatory in Gainesville (LOG), Florida. Out of the 23 strokes, 14 produced single X-ray pulses or X-ray bursts (sequences of two or more pulses), and 9 did not produce detectable X-ray emissions (with at least 128 keV energy) during 2 ms prior to and 10 μ s after the beginning of return stroke. The occurrence of X-rays was 88 and 47 % for first and subsequent strokes, respectively. The occurrence of X-rays tended to increase with increasing return-stroke peak current and decreasing distance from the lightning channel. Both these trends are expected: the return-stroke peak current is thought to be correlated with leader tip electric potential (the higher the potential, the stronger the X-ray source), and larger distances are associated with stronger X-ray absorption and scattering. Not all strokes within the same flash produced X-rays, and 5 out of 7 subsequent-stroke (dart or dart-stepped) leaders produced more X-ray pulses than their corresponding first-stroke leaders. Examples are shown in Figs. 18 and 19, where distances (r) and peak currents (I) reported by the U.S. National Lightning Detection Network (NLDN), as well as leader durations (LD) measured in electric field derivative waveforms are indicated.

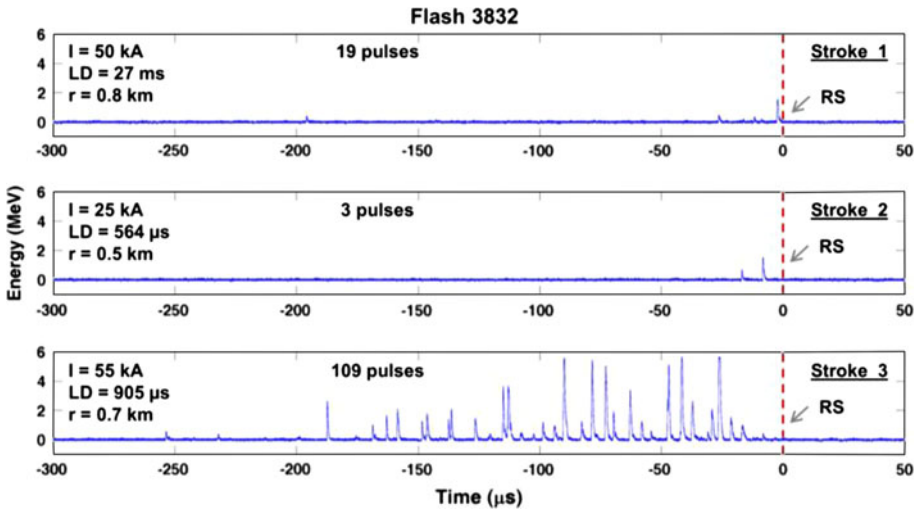


Fig. 19 X-rays produced by stroke 1 (*top*), stroke 2 (*middle*), and stroke 3 (*bottom*) of 13-stroke flash 3832. Strokes 4–13 were not recorded at LOG. NLDN-reported distances for strokes 1–3 were 0.5–0.8 km. Vertical broken lines labeled RS indicate the position of the return stroke. Some pulses seen in the plots are due to multiple photons arriving within the response time of the X-ray detector, that is, are actually each a superposition (pile-up) of two or more individual pulses. There are a total of 22 such pile-ups in the bottom panel, 3 of which are clipped at 5.6 MeV level. All discernible individual pulses are included in the pulse count given on the plots. Adapted from Mallick et al. (2012)

In Fig. 18, out of five strokes recorded at LOG, only three (of order 1, 3, and 5) produced detectable X-rays. Although the NLDN-reported distances to the five strokes ranged from 0.9 to 1.4 km, these strokes probably occurred in the same channel. This is because all subsequent-leader durations were of the order of hundreds of microseconds, which is indicative of dart or very fast dart-stepped leaders (e.g., Rakov and Uman 1990). It appears from the non-detection of X-rays during strokes 2 and 4, while strokes 1, 3, and 5 (presumably in the same channel) produced pronounced X-ray bursts, that the runaway breakdown (the only viable source of X-rays) is not a necessary feature of lightning leaders. Further, subsequent-stroke leaders shown in Fig. 18 appeared to produce more X-ray pulses (7 and 11) than their corresponding first-stroke leader (only 3 detectable X-ray pulses). It is important to note that some pulses seen in Fig. 18 (and in Fig. 19) are due to multiple photons arriving within the response time (about 1 μ s) of the X-ray detector, that is, are actually each a superposition (pile-up) of two or more individual pulses. All discernible individual pulses are included in the pulse count given in Fig. 18 (and in Fig. 19).

In Fig. 19, all three strokes recorded at LOG produced X-rays, but the third stroke was much more prolific X-ray producer (a total of 109 discernible pulses) than the other two strokes (19 and 3 pulses). Note that all three strokes apparently occurred in the same channel and that NLDN-reported peak currents for strokes 1 and 3 were similar (50 and 55 kA, respectively). This latter observation is important, since it apparently supports the theory (Cooray et al. 2009, 2010), according to which a warm, low-density channel traversed by subsequent-stroke leaders is more conducive to occurrence of the cold runaway breakdown than the virgin air in which first-stroke leaders have to develop. This observation may also have implications for production of terrestrial gamma-ray flashes (TGFs).

Mallick et al. (2012) found that, for the same leader near ground, some steps are accompanied by detectable X-ray emissions, while others are not. One possible explanation of this observation is beaming of the source electrons (different for different steps or segments of the leader channel). However, Saleh et al. (2009) found, for triggered-lightning leaders, that the source electrons are probably emitted isotropically. Another explanation is that electric field enhancements (>30 MV/m or so for the case of normal air density), needed for the cold runaway breakdown, are very brief and highly localized, so that in many cases, a sufficiently energetic electron from the tail of the bulk distribution may be unavailable to start the runaway process. This, along with the non-detection of X-rays from some strokes, while other strokes in the same channel did produce pronounced X-ray bursts, implies that the cold runaway breakdown is not a necessary feature of lightning leaders.

There appears to be a significant difference between first and subsequent leaders in terms of the distribution of X-ray source heights. Mallick et al. (2012) estimated that the maximum source height for first leaders did not exceed 800 m, whereas for subsequent leaders, the source height distribution appeared to extend to about 3.6 km.

9 Concluding Remarks

There has been significant recent progress in our understanding of lightning processes. Much of that progress has been made possible via the use of relatively new tools, such as high-speed video cameras with frame integration times ranging from a few milliseconds to a few microseconds and modern lightning locating systems. Also important is the use of rocket-triggered lightning as a partially controlled analog of natural cloud-to-ground lightning. Many recent insights into natural lightning processes would not have been possible without triggered lightning. In spite of the progress made, many aspects of lightning physics are still poorly understood or are a subject of debate. These include the dominant lightning initiation mechanism, the role of cosmic rays and energetic radiation in electrical breakdown processes in different parts of the atmosphere, properties of positive and bipolar lightning (not covered by this relatively brief review), and details of the break-through phase of the lightning attachment process, to name a few. Clearly, more efforts, both experimental and theoretical, of the physicists, atmospheric and space electricians, meteorologists, and electrical engineers are needed.

Acknowledgments This paper is largely based on the Tutorial Lecture given by the author at the Thunderstorm Effects on the Atmosphere–Ionosphere System (TEA – IS) Summer School in Torremolinos, Malaga, Spain, June 17–22, 2012, funded by the European Science Foundation (ESF). The work was also supported in part by the U.S. National Science Foundation and DARPA. Yanan Zhu helped with preparation of the figures. Two anonymous reviewers provided useful comments.

References

- Bazelyan EM, Raizer YuP (2000) *Lightning physics and lightning protection*, 325 p. IOP, Bristol
- Bazelyan EM, Gorin BN, Levitov VI (1978) *Physical and engineering foundations of lightning protection*, 223 p. Gidrometeoizdat, Leningrad
- Beasley WH, Uman MA, Rustan PL (1982) Electric fields preceding cloud-to-ground lightning flashes. *J Geophys Res* 87:4883–4902
- Betz HD, Schumann U, Laroche P (eds) (2009) *Lightning: principles, instruments and applications*. Springer, 691 p

- Biagi CJ, Jordan DM, Uman MA, Hill JD, Beasley WH, Howard J (2009) High-speed video observations of rocket-and-wire initiated lightning. *Geophys Res Lett* 36:L15801. doi:[10.1029/2009GL038525](https://doi.org/10.1029/2009GL038525)
- Biagi CJ, Uman MA, Hill JD, Jordan DM, Rakov VA, Dwyer JR (2010) Observations of stepping mechanisms in a rocket-and-wire triggered lightning flash. *J Geophys Res* 115:D23215. doi:[10.1029/2010JD014616](https://doi.org/10.1029/2010JD014616)
- Brook M, Ogawa T (1977) The cloud discharge. In R. Golde (ed) *Lightning*, vol. 1, Physics of lightning. Academic Press, London, pp. 191–230
- Chen M, Takagi N, Watanabe T, Wang D, Kawasaki Z-I, Liu X (1999) Spatial and temporal properties of optical radiation produced by stepped leaders. *J Geophys Res* 104:27573–27584
- Cooray GV (ed) (2003) *The lightning flash*, 574 p. The Institution of Electrical Engineers, London
- Cooray V, Becerra M, Rakov VA (2009) On the electric field at the tip of dart leaders in lightning flashes. *J Atmos Solar-Terr Phys* 71(12):1397–1404. doi:[10.1016/j.jastp.2009.06.002](https://doi.org/10.1016/j.jastp.2009.06.002)
- Cooray V, Dwyer JR, Rakov VA, Rahman M (2010) On the mechanism of X-ray production by dart leaders of lightning flashes. *J Atmos Solar-Terr Phys* 72(11–12):848–855. doi:[10.1016/j.jastp.2010.04.006](https://doi.org/10.1016/j.jastp.2010.04.006)
- Dwyer JR, Babich LP (2011) Low-energy electron production by relativistic runaway electron avalanches in air. *J Geophys Res* 116:A09301. doi:[10.1029/2011JA016494](https://doi.org/10.1029/2011JA016494)
- Dwyer JR, Babich L (2012) Reply to comment by A. V. Gurevich et al. on “Low-energy electron production by relativistic runaway electron avalanches in air”. *J Geophys Res* 117:A04303. doi:[10.1029/2011JA017487](https://doi.org/10.1029/2011JA017487)
- Dwyer JR, Schaal M, Rassoul HK, Uman MA, Jordan DM, Hill D (2011) High-speed X-ray images of triggered lightning dart leaders. *J Geophys Res* 116:D20208. doi:[10.1029/2011JD015973](https://doi.org/10.1029/2011JD015973)
- Eidelman S et al (2004) Review of particle physics. *Phys Lett B* 592:1–1109. doi:[10.1016/j.physletb.2004.06.001](https://doi.org/10.1016/j.physletb.2004.06.001)
- Gorin BN, Levitov VI, Shkilev AV (1976) Some principles of leader discharge of air gaps with a strong non-uniform field. *Gas discharges*. IEE Conf Publ 143:274–278
- Griffiths RF, Phelps CT (1976a) The effects of air pressure and water vapour content on the propagation of positive corona streamers, and their implications to lightning initiation. *Q J Roy Meteor Soc* 102:419–426
- Griffiths RF, Phelps CT (1976b) A model of lightning initiation arising from positive corona streamer development. *J Geophys Res* 31:3671–3676
- Gurevich AV, Zybin KP (2001) Runaway breakdown and electric discharges in thunderstorms. *Physics–Uspekhi* 44 (11): 1119–1140
- Gurevich AV, Milikh GM, Roussel-Dupre R (1992) Runaway electron mechanism of air breakdown and preconditioning during a thunderstorm. *Phys Lett A* 165:463–468
- Gurevich AV, Zybin KP, Roussel-Dupre RA (1999) Lightning initiation by simultaneous effect of runaway breakdown and cosmic ray showers. *Phys Lett A* 254:79–87
- Gurevich AV, Duncan LM, Medvedev YuV, Zybin KP (2002) Radio emission due to simultaneous effect of runaway breakdown and extensive atmospheric showers. *Phys Lett A* 301:320–326
- Gurevich AV, Duncan LM, Karashtin AN, Zybin KP (2003) Radio emission of lightning initiation. *Phys Lett A* 312:228–237
- Gurevich AV, Roussel-Dupre R, Zybin KP, Milikh GM (2012) Comment on “Low-energy electron production by relativistic runaway electron avalanches in air” by J. R. Dwyer and L. P. Babich. *J Geophys Res* 117:A04302. doi:[10.1029/2011JA017431](https://doi.org/10.1029/2011JA017431)
- Haddad MA, Rakov VA, Cummer SA (2012) New measurements of lightning electric fields in Florida: waveform characteristics, interaction with the ionosphere, and peak current estimates. *J Geophys Res* 117:D10101. doi:[10.1029/2011JD017196](https://doi.org/10.1029/2011JD017196)
- Hill JD, Uman MA, Jordan DM (2011) High-speed video observations of a lightning stepped leader. *J Geophys Res* 116:D16117. doi:[10.1029/2011JD015818](https://doi.org/10.1029/2011JD015818)
- Inan US, Cummer SA, Marshall RA (2010) A survey of ELF and VLF research of lightning-ionosphere interactions and causative discharges. *J Geophys Res* 115:A00E36. doi:[10.1029/2009JA014775](https://doi.org/10.1029/2009JA014775)
- Jayakumar V, Rakov VA, Miki M, Uman MA, Schnetzer GH, Rambo KJ (2006) Estimation of input energy in rocket-triggered lightning. *Geophys Res Lett* 33:L05702. doi:[10.1029/2005GL025141](https://doi.org/10.1029/2005GL025141)
- Krehbiel PR, Rioussel JA, Pasko VP, Thomas RJ, Rison W, Stanley MA, Edens HE (2008) Upward electrical discharges from thunderstorms. *Nature Geosci* 1:233–237. doi:[10.1038/ngeo162](https://doi.org/10.1038/ngeo162)
- Krider EP, Dawson GA, Uman MA (1968) The peak power and energy dissipation in a single-stroke lightning flash. *J Geophys Res* 73:3335–3339
- Larigaldie S, Roussaud A, Jecko B (1992) Mechanisms of high-current pulses in lightning and long-spark. *J Appl Phys* 72(5):1729–1739
- Lebedev VB, Feldman GG, Gorin BN, Shcherbakov Yu V, Syssoev VS, Rakov VA, Uman MA, Olsen RC (2007) Test of the image converter camera complex for research of discharges in long air gaps and

- lightning. In Proceedings of the 13th international conference on atmospheric electricity, Beijing, China, August 13–17, 2007, pp. 509–512
- Loeb LB (1966) The mechanisms of stepped and dart leaders in cloud-to-ground lightning strokes. *J Geophys Res* 71:4711–4721
- Lu G et al (2011) Lightning development associated with two negative gigantic jets. *Geophys Res Lett* 38:L12801. doi:[10.1029/2011GL047662](https://doi.org/10.1029/2011GL047662)
- Malan DJ, Schonland BFF (1951) The electrical processes in the intervals between the strokes of a lightning discharge. *Proc Roy Soc (Lond)* A206:145–163
- Mallick S, Rakov VA, Dwyer JR (2012) A study of X-ray emissions from thunderstorms with emphasis on subsequent strokes in natural lightning. *J Geophys Res* 117:D16107. doi:[10.1029/2012JD017555](https://doi.org/10.1029/2012JD017555)
- Moss G, Pasko VP, Liu N, Veronis G (2006) Monte Carlo model for analysis of thermal runaway electrons in streamer tips in transient luminous events and streamer zones of lightning leaders. *J Geophys Res* 111:A02307. doi:[10.1029/2005JA011350](https://doi.org/10.1029/2005JA011350)
- Nag A, Rakov VA (2008) Pulse trains characteristic of preliminary breakdown in cloud-to-ground lightning that are not followed by return stroke pulses. *J Geophys Res* 113:D01102. doi:[10.1029/2007JD008489](https://doi.org/10.1029/2007JD008489)
- Nag A, Rakov VA (2009) Some inferences on the role of lower positive charge region in facilitating different types of lightning. *Geophys Res Lett* 36:L05815. doi:[10.1029/2008GL036783](https://doi.org/10.1029/2008GL036783)
- Nag A, Rakov VA (2010a) Compact intracloud lightning discharges: 1. Mechanism of electromagnetic radiation and modeling. *J Geophys Res* 115:D20102. doi:[10.1029/2010JD014235](https://doi.org/10.1029/2010JD014235)
- Nag A, Rakov VA (2010b) Compact intracloud lightning discharges: 2. Estimation of electrical parameters. *J Geophys Res* 115:D20103. doi:[10.1029/2010JD014237](https://doi.org/10.1029/2010JD014237)
- Nag A, Rakov VA, Tsalikis D, Cramer JA (2010) On phenomenology of compact intracloud lightning discharges. *J Geophys Res* 115:D14115. doi:[10.1029/2009JD012957](https://doi.org/10.1029/2009JD012957)
- Nguyen MD, Michnowski S (1996) On the initiation of lightning discharge in a cloud 2. The lightning initiation on precipitation particles. *J Geophys Res* 101:26675–26680
- Paxton AH, Gardner RL, Baker L (1986) Lightning return stroke: a numerical calculation of the optical radiation. *Phys Fluids* 29:2736–2741
- Paxton AH, Baker L, Gardner RL (1987) Reply to comments of Hill. *Phys Fluids* 30:2586–2587
- Phelps CT (1974) Positive streamers system intensification and its possible role in lightning initiation. *J Atmos Terr Phys* 36:103–111
- Pierce ET (1958) Some topics in atmospheric electricity. In: Smith LG (ed) Recent advances in atmospheric electricity. Pergamon, New York, pp 5–16
- Qie X, Jiang R, Wang C, Yang J, Wang J, Liu D (2011) Simultaneously measured current, luminosity, and electric field pulses in a rocket-triggered lightning flash. *J Geophys Res* 116:D10102. doi:[10.1029/2010JD015331](https://doi.org/10.1029/2010JD015331)
- Rakov VA (1998) Some inferences on the propagation mechanisms of dart leaders and return strokes. *J Geophys Res* 103:1879–1887
- Rakov VA, Uman MA (2003) Lightning: physics and effects. Cambridge University Press, 687 p
- Rakov VA (2006) Initiation of lightning in thunderclouds. In Sergeev AM (ed) Topical problems of non-linear wave physics. Proceedings SPIE, Vol. 5975, pp 362–373
- Rakov VA, Uman MA (1990) Waveforms of first and subsequent leaders in negative lightning flashes. *J Geophys Res* 95(D10):16561–16577. doi:[10.1029/JD095iD10p16561](https://doi.org/10.1029/JD095iD10p16561)
- Rakov VA, Uman MA, Jordan DM, Priore CA III (1990) Ratio of leader to return stroke field change for first and subsequent lightning strokes. *J Geophys Res* 95(16):579–587
- Rakov VA, Thottappillil R, Uman MA, Barker PP (1995) Mechanism of the lightning M component. *J Geophys Res* 100:25701–25710
- Rakov VA, Uman MA, Rambo KJ, Fernandez MI, Fisher RJ, Schnetzer GH, Thottappillil R, Eybert-Berard A, Berlandis JP, Lalande P, Bonamy A, Laroche P, Bondiou-Clergerie A (1998) New insights into lightning processes gained from triggered-lightning experiments in Florida and Alabama. *J Geophys Res* 103:14117–14130
- Rao M, Bhattacharya H (1966) Lateral corona currents from the return stroke channel and slow field change after the return stroke in a lightning discharge. *J Geophys Res* 71:2811–2814
- Saleh Z, Dwyer J, Howard J, Uman M, Bakhtiari M, Concha D, Stapleton M, Hill D, Biagi C, Rassoul H (2009) Properties of the X-ray emission from rocket-triggered lightning as measured by the Thunderstorm Energetic Radiation Array (TERA). *J Geophys Res* 114:D17210. doi:[10.1029/2008JD011618](https://doi.org/10.1029/2008JD011618)
- Solomon R, Schroeder V, Baker MB (2001) Lightning initiation: conventional and runaway-breakdown hypotheses. *Q J R Meteorol Soc* 127:2683–2704
- Solomon R, Adamo C, Baker MB (2002) A lightning initiation mechanism: application to a thunderstorm electrification model. *C R Physique* 3:1325–1333

- Somu VB, Rakov VA, Haddad MA, Cummer SA (2012) Ionospheric reflection heights for wideband electric fields produced by consecutive return strokes within the same lightning flash. Abstract AE43A-0241, presented at 2012 fall meeting, AGU, San Francisco, Calif., December 3–7, 2012
- Wang D, Rakov VA, Uman MA, Takagi N, Watanabe T, Crawford DE, Rambo KJ, Schnetzer GH, Fisher RJ, Kawasaki Z-I (1999a) Attachment process in rocket-triggered lightning strokes. *J Geophys Res* 104:2143–2150
- Wang D, Takagi N, Watanabe T, Rakov VA, Uman MA (1999b) Observed leader and return-stroke propagation characteristics in the bottom 400 m of a rocket-triggered lightning channel. *J Geophys Res* 104:14369–14376
- Yashunin SA, Mareev EA, Rakov VA (2007) Are lightning M components capable of initiating sprites and sprite halos? *J Geophys Res* 112:D10109. doi:[10.1029/2006JD007631](https://doi.org/10.1029/2006JD007631)
- Yoshida S, Biagi CJ, Rakov VA, Hill JD, Stapleton MV, Jordan DM, Uman MA, Morimoto T, Ushio T, Kawasaki Z-I, Akita M (2012) The initial stage processes of rocket-and-wire triggered lightning as observed by VHF interferometry. *J Geophys Res* 117:D09119. doi:[10.1029/2012JD017657](https://doi.org/10.1029/2012JD017657)